2026 IEEE/SICE International Symposium on System Integration (SII)
January 11-14, 2026. Cancún, México

Evaluation of Developed Structures for Drone Audition-purposed Measurement Equipment in Actual Flight Conditions

Yuta Tsukamoto[1] and Kotaro Hoshiba[1]

Abstract— **Auditory scene analysis using drones, a technology known as "drone audition", is a promising method for locating survivors in disaster areas. This technology requires a structure to mount measurement equipment onto the drone. A previous study proposed a versatile structure designed to be attached to the drone's landing gear and evaluated its applicability based on four criteria: mass limitation, load capacity, vibration characteristics, and ease of adjustment. As for vibration characteristics, it was confined to the theoretical evaluation and was required to be evaluated under actual flight conditions. In this research, we evaluate the vibration characteristics of the structure during flight by comparing acceleration responses at several points on the conventional and proposed structures. The results confirmed that the proposed structure's vibration characteristics are superior to the conventional one's for minimizing the impact on the measurement equipment during flight. Furthermore, it was found that the proposed structure exhibits larger vibrations than the conventional one upon landing. This is acceptable, since acoustic measurements are not performed during landing. Therefore, it became clear that the proposed structure must have sufficient strength to withstand the impact force during landing.**

I. INTRODUCTION

The application of drones to search and rescue operations in disaster areas is highly anticipated due to their rapid deployment capabilities and high maneuverability. Many search technologies have focused on visual information from drone-mounted cameras [1–5]. However, these visual-based systems are ineffective under poor lightning conditions or when victims are buried in rubble. To solve this problem, audio-based search technologies using drone-mounted microphones have been studied [6–11]. This technology is an application of "Drone Audition", a research field focused on auditory scene analysis using drone-mounted microphones, and is performed by localizing human-related sounds. The practical application of drone audition requires a structure for mounting its essential equipment, such as a microphone array and a small processing unit. This structure must be designed within the payload capacity of the drone. In general, this has led to the development of dedicated structures designed to be directly affixed to the body of a specific drone. This approach suffers from poor versatility, as each structure must be redesigned to accommodate the specific shape and dimensions of each drone. As a result, the engineering and manufacturing costs associated with these non-transferable structures pose a significant obstacle to the implementation of drone audition technology.

[1]All authors are with the Department of Mechanical Engineering, School of Engineering, Institute of Science Tokyo, 2-12-1 Ookayama, Meguro-ku, Tokyo 152-8550, Japan, {tsukamoto.y.ak, hoshiba.k.aa}@m.titech.ac.jp

In our previous study, we focused on the common use of inverted T-shaped landing gear in many industrial drones and proposed a structure that could be easily attached to drones of various sizes [12]. Specifically, the proposed structure was designed to attach to the landing gear rather than the drone's main body, allowing for installation on drones of different sizes with only minimal adjustments. We then designed the structure based on four criteria and evaluated its performance accordingly. First, the mass limitation was evaluated by measuring the mass of the fabricated structure and comparing it to the payloads capacities of multiple drones. Second, the load capacity was evaluated by conducting a static load analysis based on the Finite Element Method (FEM). Third, the vibration characteristics was evaluated by eigenvalue analysis using FEM. Fourth, the ease of adjustment was evaluated by fitting the fabricated structure onto multiple drones. These evaluations confirmed that the proposed structure satisfied these four design criteria. However, the assessment of load capacity and vibration characteristics was confined to numerical analysis via FEM. The structure's load capacity can be appropriately evaluated using static load analysis with loads incorporating sufficient safety factors and based on the mass of the mounted measurement equipment. On the other hand, the structure's vibration characteristics are likely influenced by factors such as dimensional and assembly errors of the actual components, as well as by the effects of fastening joints. Therefore, we concluded that evaluating the structure's vibration characteristics under actual flight conditions, in addition to eigenvalue analysis of the standalone structure.

Therefore, in this study, we measured actual acceleration responses during outdoor flight in three configurations: the drone without a structure, the drone with the conventional structure attached directly to the bottom of the drone's body, and the drone with the proposed structure attached to the drone's landing gear. From these results, we evaluated the vibration characteristics of the structure during flight by comparing acceleration responses at several points on the conventional and proposed structures.

II. DESIGN OF THE STRUCTURE

Leveraging the commonly used inverted T-shaped landing gear found on many industrial drones (Fig. 1(a)), we have developed a versatile structure for mounting measurement equipment as shown in Fig. 1(b). As detailed in Fig. 2, the proposed structure is a truss-like assembly of short pipes that attaches directly to the landing gear and supports a long pipe for mounting measurement equipment. A key advantage of this design is its adjustability: it can be fitted to drones of

978-1-6654-5784-2/26/$31.00 ©2026 IEEE

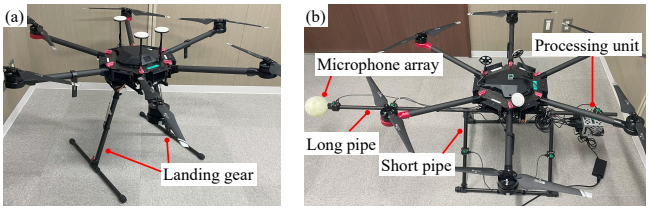

Fig. 1. Appearance of the drone and structure: (a) drone without a structure, (b) drone with the proposed structure.

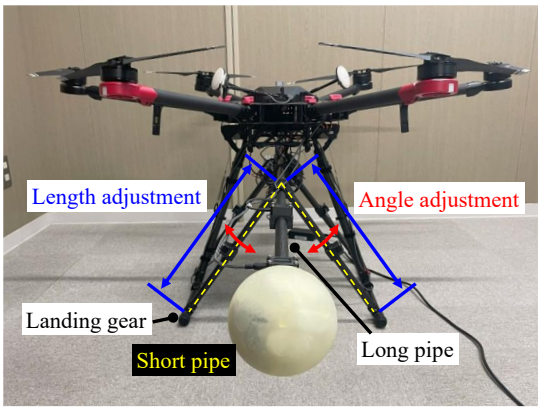

Fig. 2. Front view of the drone with the proposed structure.

various sizes simply by changing the length of the short pipes and their connecting angles.

The design of this structure must satisfy four key criteria: mass limitation, load capacity, vibration characteristics, and ease of adjustment.

1) Mass limitation
   The combined mass of the structure and the measurement equipment must be kept below the drone's maximum payload.
2) Load capacity
   The structure must be capable of supporting the static load of the measurement equipment.
3) Vibration characteristics
   The structure must be designed with appropriate vibration characteristics to prevent resonance and fatigue failure caused by rotor vibrations during flight.
4) Ease of adjustment
   Placing the microphone array at a distance from the drone's body is necessary to reduce rotor ego-noise, but this unbalances the drone's overall center of gravity. To compensate for this imbalance, the position of the processing unit must be adjusted along the long pipe. This necessitates a design where measurement equipment can be easily repositioned on the structure.

The main structure for this study was built with CFRP (Carbon Fiber Reinforced Plastics) pipes (20 mm outer diameter, 1 mm wall thickness). The connecting joints were designed as solid parts and 3D-printed from a nylon plastic filament reinforced with short carbon fibers (Onyx, Markforged) [13].

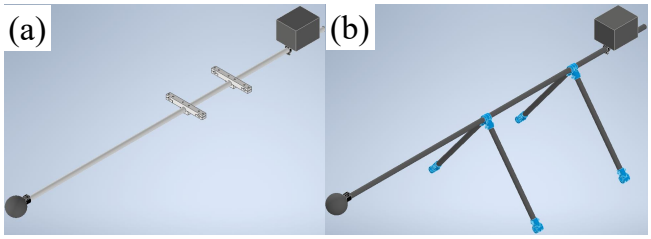

Fig. 3. Models for eigenvalue analysis: (a) the conventional structure, (b) the proposed structure.

III. NUMERICAL VIBRATION ANALYSIS

In a previous study, the design criteria for the structure presented in the previous chapter were evaluated for application on Matrice 210 RTK V2 (DJI) [14]. This chapter re-evaluates these criteria for a larger drone, Matrice M600 Pro (DJI) [15]. Three of these criteria, mass limitation, load capacity, and ease of adjustment, are considered to have already been adequately validated by our previous study.

The mass limitation is considered met because Matrice M600 Pro's payload capacity (5.50 kg) far exceeds that of Matrice 210 RTK V2 (1.23 kg), while the structure's mass remains largely unchanged. The load capacity can be assessed using the same FEM-based static load analysis as before, since the mounted measurement equipment is identical. The ease of adjustment is also deemed satisfactory as the fundamental design of the structure is the same as in the previous study.

In contrast, the structure's vibration characteristics require re-evaluation because they are highly dependent on the drone's size, as the length and angles of the short pipes must be changed to accommodate different drones. Therefore, it is necessary to evaluate the structure using the specific geometry and dimensions designed for the target drone. Accordingly, we evaluated the designed structure via eigenvalue analysis using FEM software (Inventor Nastran, Autodesk).

A. *Conditions for eigenvalue analysis*

For comparison, we developed finite element models for two configurations, as shown in Fig. 3: the conventional structure attached directly to the component on the bottom of the drone's body, and our proposed structure attached to the landing gear. Both models include the microphone array and the processing unit. In these models, the CFRP pipes were represented by shell elements and the 3D printed parts by solid elements. Boundary conditions were constrained at the contact surfaces: between the conventional structure and the bottom of the drone's body, and between the proposed structure and the landing gear. Table I lists the mechanical properties used in the eigenvalue analysis along with those in the previous study [12], [16], [17].

B. *Result of eigenvalue analysis*

Table II lists the natural frequencies for the 1st to the 10th modes in three cases: the conventional and the proposed

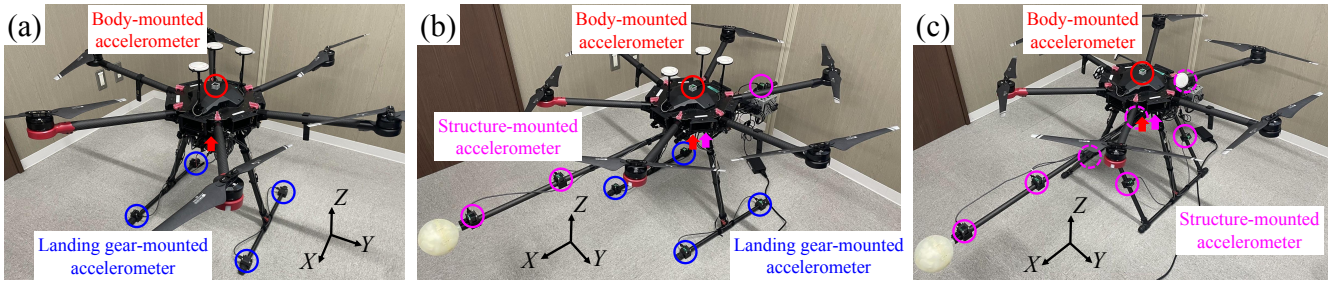

Fig. 4. Positions of accelerometers: (a) drone without a structure, (b) drone with the conventional structure, (c) drone with the proposed structure. The red, blue, and magenta circles represent the accelerometers arranged on the drone's main body, the landing gear, and the structure, respectively.

TABLE I

MECHANICAL PROPERTIES USED FOR NUMERICAL ANALYSIS.

	CFRP pipe	Onyx
Density [kg/m^3]	1550	1139
Young's modulus (E_x) [GPa]	113.6	1.20
Young's modulus (E_y, E_z) [GPa]	113.6	0.85
Poisson's ratio (ν_{xy}, ν_{yz}, ν_{zx})	0.3	0.35
Transverse modulus (G_{xy}) [GPa]	43.7	0.67
Transverse modulus (G_{yz}) [GPa]	43.7	0.47
Transverse modulus (G_{zx}) [GPa]	43.7	0.39

TABLE II

NATURAL FREQUENCIES OF THE CONVENTIONAL STRUCTURE AND THE PROPOSED STRUCTURE.

	Matrice M600 Pro		Matrice 210 RTK V2
	Conventional	Proposed	Proposed
1st	14.3	17.3	21.9
2nd	15.5	17.5	22.4
3rd	24.3	32.7	70.7
4th	27.4	37.9	82.9
5th	109.5	48.9	134.4
6th	131.7	118.8	199.9
7th	165.0	215.0	269.3
8th	182.8	218.0	277.1
9th	275.0	281.6	301.1
10th	280.2	309.0	476.7

structures applied to Matrice M600 Pro, and the proposed structure applied to Matrice 210 RTK V2. From these results, it is evident that the natural frequencies of the structure applied to Matrice 210 RTK V2 differ significantly from those of Matrice M600 Pro. This indicates the necessity of evaluating a model specifically configured for the target drone.

IV. VIBRATION EVALUATION IN ACTUAL FLIGHT CONDITIONS

In this section, we evaluate the the vibration characteristics of structures in actual flight conditions. For this evaluation, the fully equipped structure was mounted on the drone, and the acceleration responses were measured at several locations on the drone's main body, the landing gear, and the structure.

A. Measurement condition

Vibration characteristics were evaluated under three configurations as shown in Fig.4: the drone without a structure, the drone with the conventional structure attached to the bottom of the drone's main body, and the drone with the proposed structure mounted on the landing gear. The accelerometers were arranged on the drone ' s main body, the landing gear, and the structure. For each configuration, acceleration responses were measured during seven flight maneuvers: moving (upward, downward, forward, leftward), hovering, takeoff, and landing), considering the drone's symmetry. The coordinate system was defined as *X*-axis (forward), *Y*-axis (leftward), and *Z*-axis (vertical). Acceleration responses were obtained using an MPU6886 accelerometer in an M5Stack ATOM Matrix. The measurements were performed at a sampling frequency of 1 kHz over a 5 seconds duration, providing a frequency resolution of 0.2 Hz in the analysis.

B. Measurement result

The structure's vibration characteristics in actual flight conditions were evaluated by comparing acceleration responses from key locations based on six perspectives.

1) Effect of flight conditions: To identify a representative flight condition for evaluation, acceleration responses measured at the top surface of the drone without a structure were compared under five flight conditions: moving (upward, downward, forward, leftward) and hovering. Fig. 5 and Fig. 6 show the frequency spectra of these measurements. In Fig. 5, the blue, green, and red lines represent the data when moving upward, moving downward, and hovering, respectively. Similarly, in Fig. 6, they represent the data when moving forward, moving leftward, and hovering, respectively. In the *X* and *Y*-axis directions, vibrations remain small across all flight conditions, with minimal differences between them. In the *Z*-axis direction, while the characteristics are also similar, some differences appear around 220 Hz depending on the flight condition. However, since the same peak frequencies occur in all directions regardless of the maneuver, the influence of the flight condition on the overall vibration characteristics was considered to be minor. Therefore, for all subsequent comparisons, the vibration characteristics during hovering were used as the representative case.

2) Comparison of vibration at the drone's body and its landing gear: For the drone without a structure, acceleration responses obtained at the top and bottom of the drone's main body and at the tips of the landing gear during hovering were compared. Fig. 7 shows the frequency spectra of these

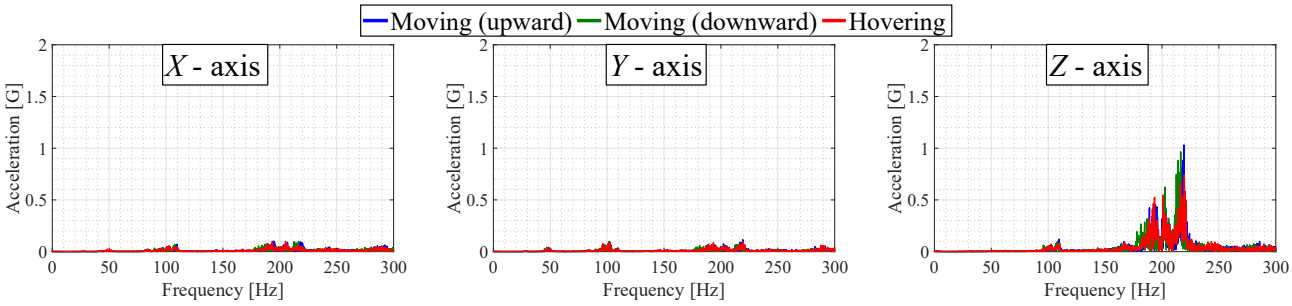

Fig. 5. Frequency spectra of obtained acceleration responses at the top of the drone's main body without a structure under different flight conditions (moving (upward, downward) and hovering).

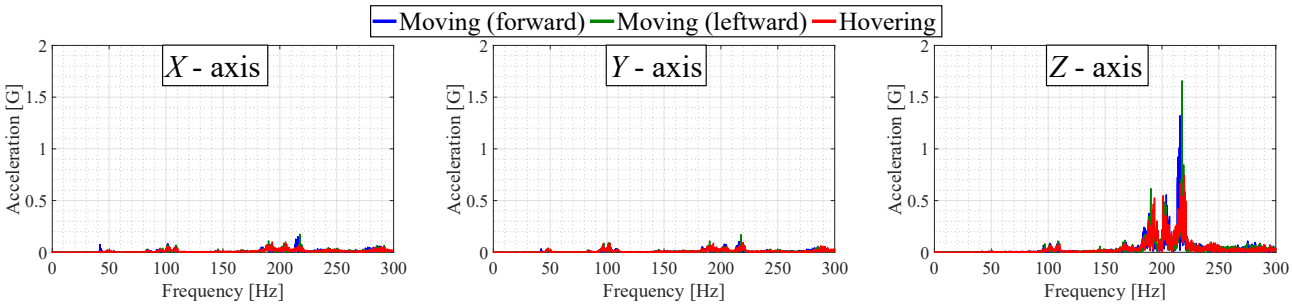

Fig. 6. Frequency spectra of obtained acceleration responses at the top of the drone's main body without a structure under different flight conditions (moving (forward, leftward) and hovering).

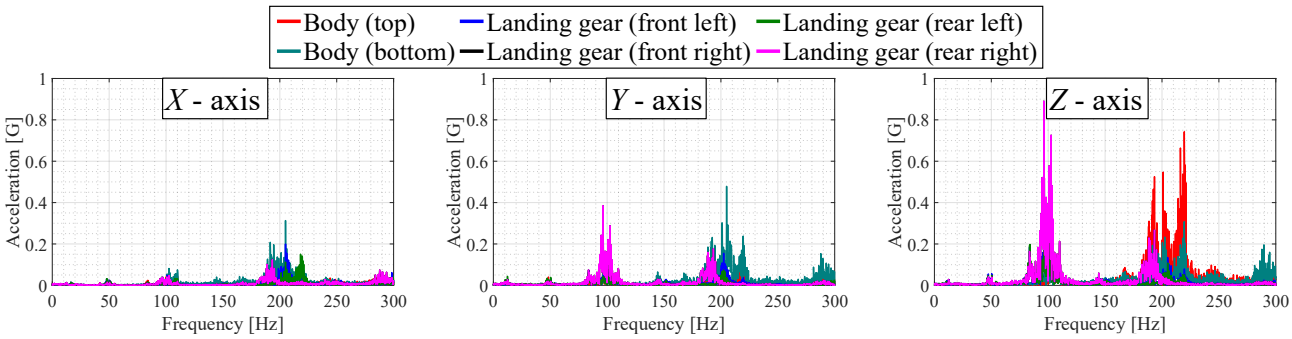

Fig. 7. Frequency spectra of obtained acceleration responses at the top and bottom of the drone's main body and at the four tips (front left, rear left, front right, and rear right) of the landing gear without a structure during hovering.

measurements. In this figure, the red and light blue lines represent the data at the drone's top and bottom surfaces, respectively, while the blue, green, black, and magenta lines represent the data at the tips of the landing gear. In all directions, the vibrations at the tips of the landing gear are significantly larger than those on the drone's main body, with prominent peaks observed around 100 Hz in the Y and Z-axis directions. This is considered to be due to the free ends of the drone's landing gear, which amplify vibrations originating from the drone's main body. An exception occurs in the Z-axis direction at 220 Hz, where large vibrations occur on the top and bottom surfaces of the drone's main body, presumed to be an effect of rotor vibration.

3) Vibrational relationship between the drone's main body and the tip of the attached conventional structure: The vibrational relationship between the drone's main body without a structure and the tip of the attached conventional structure was evaluated. Figure 8 shows the frequency spectra of these measurements. The blue and red lines represent the data at the bottom of the drone and the tip of the attached conventional structure, respectively. The conventional structure's natural frequencies, derived from numerical analysis, are also indicated by a black dotted line. Although the structure dampens the vibration of the drone's body in all directions, a significant resonance peak is observed at its tip around 110 Hz in the Y and Z-axis directions.

This 110 Hz peak is attributed to resonance, as the frequency coincides with the natural frequency of the standalone structure. Additionally, the acceleration response in this comparison was measured at the bottom surface of the drone's main body, and may differ from the vibration occurring at the attached position of the conventional struc-

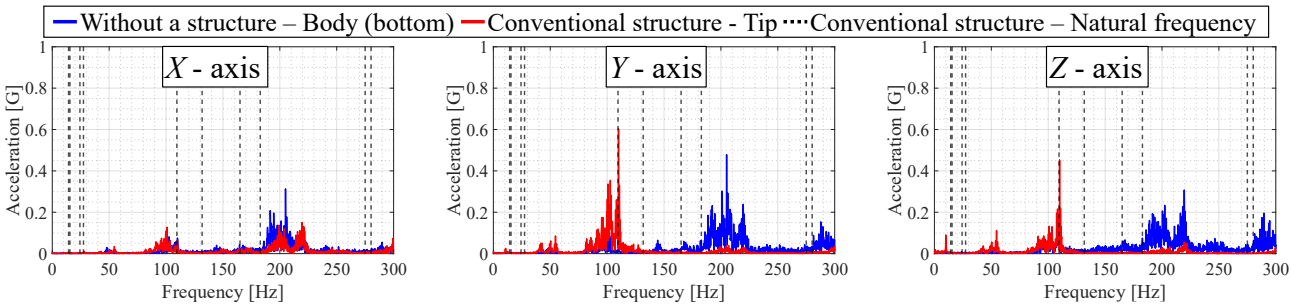

Fig. 8. Frequency spectra of obtained acceleration response at the bottom of the drone's main body without a structure and the tip of the attached conventional structure.

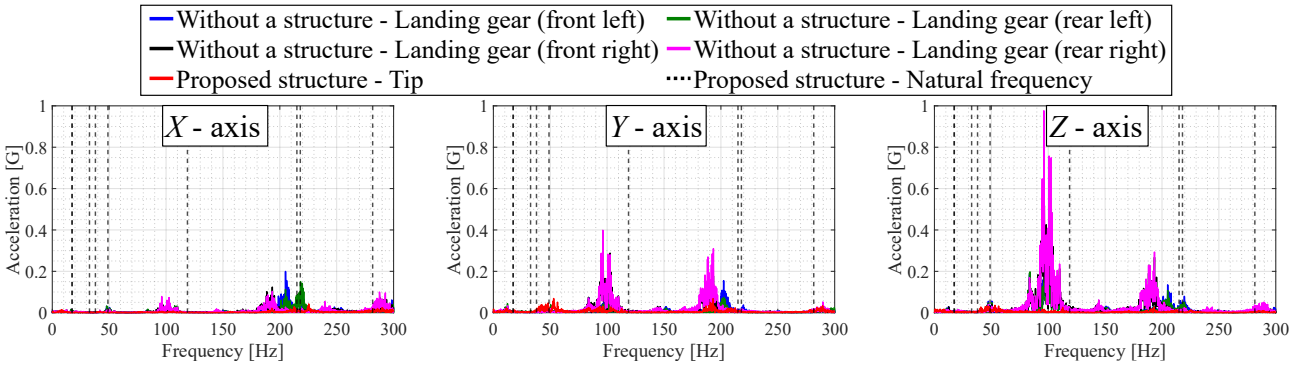

Fig. 9. Frequency spectra of obtained acceleration response at the landing gear without a structure and the tip of the attached proposed structure.

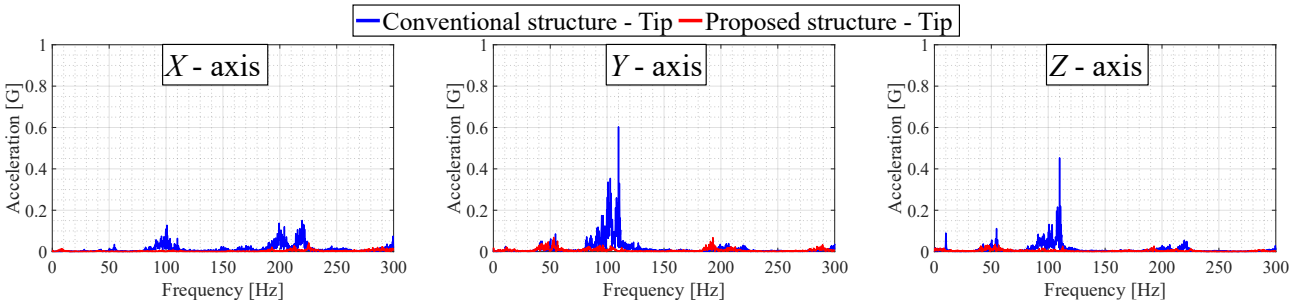

Fig. 10. Frequency spectra of obtained acceleration response at the tips of the attached conventional and proposed structures.

ture. Therefore, the combination of the structure's vibration characteristics and the different measurement locations is thought to account for the significant difference between the acceleration responses observed at the drone's main body and at the tip of the attached conventional structure.

4) Vibrational relationship between the landing gear and the tip of the attached proposed structure: The vibrational relationship between the landing gear without a structure and the tip of the attached proposed structure was evaluated. Figure 9 shows the frequency spectra of these measurements. The blue, green, black, and magenta lines represent the data at the tips of the landing gear without a structure. The red line represents the data at the tip of the attached proposed structure. The proposed structure's natural frequencies, derived from numerical analysis, are also indicated by a black dotted line. The results clearly show that the structure suppresses vibration in all directions. This is presumably because the natural frequency of the standalone proposed structure does not coincide with the peak frequencies of the landing gear without a structure. Additionally, it is considered that the mounted structure forms a truss-like configuration, which structurally dampens the vibration.

5) Comparison of vibration between the tips of both structures: The vibration characteristics at the tips of the conventional and proposed structures were evaluated. Figure 10 shows the frequency spectra of these measurements. The blue and red lines represent the data at the tips of the conventional and proposed structures, respectively. In all directions, the proposed structure suppresses vibration at its tip. These results are attributed to three primary factors. First, the landing gear's vibration at the attached position of the structure does not coincide with the proposed structure's natural frequency. Second, the proposed structure is structurally more effective at damping vibration. Third, the

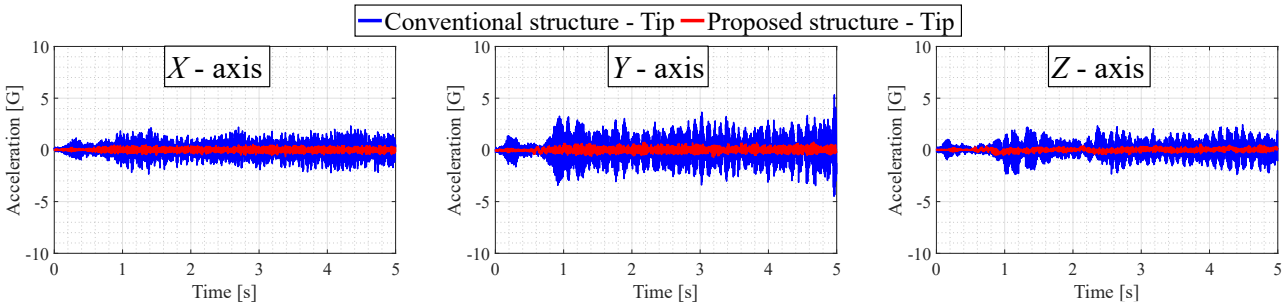

Fig. 11. Acceleration response at the tips of attached conventional and proposed structures during takeoff.

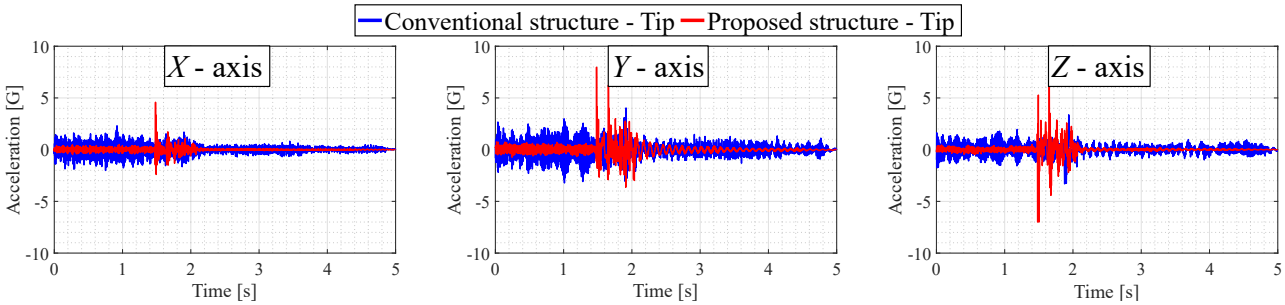

Fig. 12. Acceleration response at the tips of attached conventional and proposed structures during landing.

vibration from the rotor propagates through the landing gear, and because the distance to the structure's tip is larger, this leads to attenuation of the vibration during propagation.

6) Effects of takeoff and landing on the tip of the structure: The structures were evaluated by comparing the acceleration responses at the tips of the conventional and proposed structures during takeoff and landing. Figure 11 and Figure 12 show the acceleration responses during takeoff and landing. In each figure, the blue line represents the acceleration response at the tip of the conventional structure, while the red line represents that of the proposed structure. During takeoff, the acceleration response of the proposed structure remains relatively constant and is smaller than that of the conventional structure. This is presumably because the rotor rotation during takeoff is similar to that during the upward moving, and the measurement point is located far from the rotor. However, during landing, a large vibration is observed at the tip of the proposed structure. This is considered to be due to the landing impact acting almost directly on the tip of the proposed structure, which is attached directly to the landing gear.

The results indicate that the proposed structure is more effective than the conventional one during flight. As shown in Fig.11 and Fig.12, the acceleration response at the tip of the proposed structure is suppressed to less than 1 G in all directions during flight, which minimizes the impact on the measurement equipment. On the other hand, it is observed that the proposed structure exhibits larger vibrations than the conventional one upon landing. This characteristic is acceptable because acoustic measurements are not conducted during landing, assuming the structure has sufficient strength.

V. CONCLUSION

In this study, the vibration characteristics of a proposed versatile structure designed to be attached to the drone's landing gear for drone audition-purposed measurement equipment were evaluated in actual outdoor flight conditions. Acceleration responses were measured during seven flight conditions under three configurations: the drone without a structure, the drone with the conventional structure attached directly to the bottom of the drone's body, and the drone with the proposed structure attached to the landing gear. Comparisons of these results confirmed that the proposed structure's vibration characteristics are superior to the conventional one's for minimizing the impact on the measurement equipment during flight. Furthermore, it was found that the proposed structure exhibits larger vibrations than the conventional one upon landing. This is acceptable, since acoustic measurements are not performed during landing. Therefore, it became clear that the proposed structure must have sufficient strength to withstand the impact force during landing.

In this study, we evaluated the structural vibration response during actual outdoor flight under wind speeds of approximately 5 m/s. Based on these results, as future work, we will record the target sound during flight under similar outdoor conditions to assess the effect of flight-induced vibrations on the recorded sound. Furthermore, we plan to conduct similar evaluations in environments with stronger winds and higher environmental noise levels. These assessments will use metrics such as the signal-to-noise ratio to compare the target sound recorded by drone-mounted microphone array with that recorded by a fixed microphone array at the

same location without the drone. Additionally, our findings indicate that measures to address landing impact forces are necessary. This suggests that a mechanism designed to absorb these impacts should also be considered.

ACKNOWLEDGMENT

This work was partially supported by JSPS KAKENHI Grant No. JP22K14218 and NEXCO Group Companies ' Support Fund to Disaster Prevention Measures on Expressways.

REFERENCES

[1] P. Urbanová, M. Jurda, T. Vojtíšek, and J. Krajsa, "Using drone-mounted cameras for on-site body documentation: 3D mapping and active survey", *Forensic Science International*, vol. 281, pp. 52-62, 2017.

[2] A. Quan, C. Herrmann and H. Soliman, "Project Vulture: A Prototype for Using Drones in Search and Rescue Operations", 2019 15th International Conference on Distributed Computing in Sensor Systems (DCOSS), pp. 619–624, 2019.

[3] S. Sambolek and M. Ivasic-Kos, "Automatic Person Detection in Search and Rescue Operations Using Deep CNN Detectors", IEEE Access, vol. 9, pp. 37905–37922, 2021.

[4] B. Mishra, D. Garg, P. Narang, and V. Mishra, "Drone-surveillance for search and rescue in natural disaster", *Computer Communications*, vol. 156, pp. 1-10, 2020.

[5] T. Tuan Do, D. D. Nguyen, X. H. Ho, and V. D. Nguyen, "Leveraging Deep Learning Technique with Meta-Data-Featured Images Captured by Drone for Real-Time Victim Positioning in Flood-Affected Areas", *2025 19th International Conference on Ubiquitous Information Management and Communication (IMCOM)*, pp. 1-8, 2025.

[6] Y. Yamamoto, Z. C. Tang, K. Taguchi, and H. Tsuchiya, "Drone with Multiple Sensors for Night-time Search Missions of Disaster Victims", *2024 IEEE 19th Conference on Industrial Electronics and Applications (ICIEA)*, pp. 1-6, 2024.

[7] L. Wang and A. Cavallaro, "Deep-Learning-Assisted Sound Source Localization From a Flying Drone", *IEEE Sensors Journal*, vol. 22, no. 21, pp. 20828-20838, 2022.

[8] M. Clayton, L. Wang, A. McPherson, an A. Cavallaro, "An Embedded Multichannel Sound Acquisition System for Drone Audition", *IEEE Sensors Journal*, vol. 23, no. 12, pp. 13377-13386, 2023.

[9] K. Hoshiba, K. Washizaki, M. Wakabayashi, T. Ishiki, M. Kumon, Y. Bando, D. Gabriel, K. Nakadai, H. G. Okuno: "Design of UAV-Embedded Microphone Array System for Sound Source Localization in Outdoor Environments", *Sensors*, vol. 17, no. 11, pp. 1–16, 2017.

[10] K. Hoshiba, K. Nakadai, M. Kumon, H. G. Okuno: "'Assessment of MUSIC-Based Noise-Robust Sound Source Localization with Active Frequency Range Filtering", *Journal of Robotics and Mechatronics*, vol. 30, no. 3, pp. 426–435, 2018.

[11] K. Hoshiba, I. Komatsuzaki and N. Iwatsuki, "Proposal of Practical Sound Source Localization Method Using Histogram and Frequency Information of Spatial Spectrum for Drone Audition", *Drones*, vol. 8, no. 4, 159, 2024.

[12] Y. Tsukamoto, K. Hoshiba, and N. Iwatsuki, "Development of a Versatile Structure for Mounting Drone Audition-purposed Measurement Equipment", *2025 IEEE/SICE International Symposium on System Intergation (SII)*, pp. 1028-1033, 2025.

[13] Markforged, "Onyx" , `https://markforged.com/jp/materials/plastics/onyx` (accessed on November 11, 2025)

[14] DJI, "Support for Matrice 200 Series V2", `https://www.dji.com/support/product/matrice-200-series-v2` (accessed on November 11, 2025)

[15] DJI, "Support for Matrice 600 Pro", `https://www.dji.com/support/product/matrice600-pro` (accessed on November 11, 2025)

[16] HOPEC, "Technology", `https://www.hopec.jp/technology/` (accessed on November 11, 2025)

[17] TORAY, "Mechanical properties", `https://www.toplaseiko.com/oshidashi/data/` (accessed on November 11, 2025)